

Wave and vibration attenuation analyzes of 2-D phononic crystals using the scaled boundary finite element method

H.V. Cantanhêde¹, E.J.P. Miranda Jr.^{2,3}, J.M.C. Dos Santos⁴

¹*Federal University of Sergipe, UFS
Av. Marechal Rondon, CEP 49100-000, São Cristóvão, SE, Brazil
heliovitorcantanhede@gmail.com*

²*Federal Institute of Maranhão, IFMA-EIB-DE
Rua Afonso Pena, 174, CEP 65010-030, São Luís, MA, Brazil*

³*Federal Institute of Maranhão, IFMA-PPGEM
Avenida Getúlio Vargas, 4, CEP 65030-005, São Luís, MA, Brazil*

⁴*University of Campinas, UNICAMP-FEM-DMC
Rua Mendeleyev, 200, CEP 13083-970, Campinas, SP, Brazil.*

Abstract. This study uses the scaled boundary finite element method (SBFEM) to investigate the wave propagation and vibration in a 2-D phononic crystal (PnC). The SBFEM is a general semi-analytical method where a problem domain is divided into subdomains satisfying the scaling requirement. It offers the advantages of the finite element method (FEM) and the boundary element method (BEM), avoiding some drawbacks and making it very attractive for PnC applications. In this investigation, the SBFEM is formulated using the Bloch-Floquet theory to model the periodic 2-D PnC unit cells. The 2-D PnC is composed by square inclusions distributed in a matrix with square lattice. The SBFEM results are computed in the form of dispersion diagram and forced response of the 2-D PnC. The dispersion diagram obtained by SBFEM is validated with those obtained by the FEM and plane wave expansion (PWE) method.

Keywords: Phononic crystal, Scaled boundary finite element, Vibration attenuation, Band gaps.

1 Introduction

The study of wave propagation in periodic systems began with Brillouin [1]. He focused on problems of solid-state physics, electrical engineering, and electronics. Then, elastic wave propagation in periodic engineering structures, e.g., beams and plates, was investigated by Mead [2], Orris and Petyt [3]. In the last years, acoustic wave propagation in periodic composite materials known as phononic crystals (PCs) has attracted much attention from researchers due to its unique physical properties [4, 5]. They have received renewed attention because they exhibit band gaps, where mechanical (elastic or acoustic) waves are drastically attenuated inside the band gaps. The Bragg scattering mechanism generates the phononic crystal band gaps, which generate destructive interference among propagating waves. Bragg's law governs the frequency band location, where the wavelength is inversely related to PC unit-cell size. Different methods have been developed to compute elastic band gaps in PCs. Among them, it can be mentioned the plane wave expansion (PWE) method [6, 7], the conventional finite element method (FEM) [8], the finite difference time domain (FDTD) method [9], the boundary element method (BEM) [4], and the wave finite element (WFE) method [10, 11]. By merging the advantages of FEM and BEM, a semi-analytical approach called the scaled boundary finite element method (SBFEM) was developed. The SBFEM was initially formulated by Wolf [12] and Song [13] for modeling wave propagation in unbounded domains. Some SBFEM works have also been published in the last decade, mainly related to the wave propagation approach. In [14], the SBFEM is efficiently applied to wave propagation problems. This paper extends the SBFEM formulation to analyze the in-plane wave propagation in linear elastic periodic PCs and evaluating their efficiency when compared to FEM and PWE.

2 SBFEM for periodic systems

This section presents the formulation to model periodic structures with PC applications using the SBFEM. The mathematical formulation of the SBFEM is described for the case of an in-plane stress state, where the dynamic stiffness matrix of a PC with a periodic unit cell is obtained. The PC formulation is also described for the dispersion curves (using the Bloch-Floquet periodic boundary conditions) and forced response calculations. The differential equation in the frequency domain for the in-plane elastodynamic problem can be expressed in matrix form as:

$$\nabla^T \boldsymbol{\sigma} + \omega^2 \rho \mathbf{u} = 0, \quad (1)$$

where ρ is the mass density, ω is the circular frequency, ∇ is the differential operator matrix, $\boldsymbol{\sigma}$ is the stress vector and \mathbf{u} is the displacement vector, given by:

$$\nabla = \begin{bmatrix} \frac{\partial}{\partial \hat{x}} & 0 \\ 0 & \frac{\partial}{\partial \hat{y}} \\ \frac{\partial}{\partial \hat{y}} & \frac{\partial}{\partial \hat{x}} \end{bmatrix}, \quad \boldsymbol{\sigma} = \begin{bmatrix} \sigma_x \\ \sigma_y \\ \tau_{xy} \end{bmatrix}, \quad \mathbf{u} = u(\hat{x}, \hat{y}) = \begin{bmatrix} u_x \\ u_y \end{bmatrix}. \quad (2)$$

Since SBFEM is based entirely on FEM, but with the boundary discretization only [15], consider a two-dimensional linear elastic bounded domain V as shown in Fig. 1.

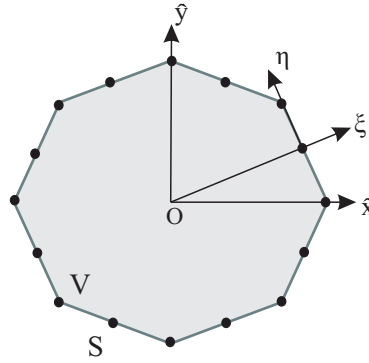


Figure 1. Scaled boundary coordinate system for a 2D bounded domain.

In the domain, V , a scaling center O is chosen in a region where the total boundary S is visible. The origin of the cartesian coordinate system (\hat{x}, \hat{y}) is selected at the scaling center, and the boundary S is discretized. The coordinates of the nodes of an element in the cartesian coordinate system are arranged in the vectors \mathbf{x} and \mathbf{y} . The geometry of an element is interpolated using the shape functions $\mathbf{N}(\eta)$ formulated in the local coordinate η as:

$$x(\eta) = \mathbf{N}(\eta)\mathbf{x}, \quad y(\eta) = \mathbf{N}(\eta)\mathbf{y}. \quad (3)$$

The geometry of the domain V is described by scaling the boundary with the dimensionless radial coordinate η pointing from the scaling center O to a point on the boundary. Then $\xi = 0$ at O and $\xi = 1$ on the chosen boundary. A point (\hat{x}, \hat{y}) inside the domain is expressed by scaling as:

$$\hat{x}(\xi, \eta) = \xi \mathbf{N}(\eta)\mathbf{x}, \quad \hat{y}(\xi, \eta) = \xi \mathbf{N}(\eta)\mathbf{y}, \quad (4)$$

where η and ξ are the scaled boundary coordinates, and $0 \leq \xi \leq 1$ are from the scaling center to the boundary. After expressing the governing differential equations in the scaled boundary coordinates, the displacement is expressed as [15]:

$$\mathbf{E}_0 \xi^2 \mathbf{u}(\xi)_{,\xi\xi} + ((s-1)\mathbf{E}_0 - \mathbf{E}_1 + \mathbf{E}_1^T) \xi \mathbf{u}(\xi)_{,\xi} + ((s-2)\mathbf{E}_1^T - \mathbf{E}_2) \mathbf{u}(\xi) + (\omega \xi)^2 \mathbf{M}_0 \mathbf{u}(\xi) = 0, \quad (5)$$

where $s = 2$ or $s = 3$ denotes the spatial dimension of the domain, and ω is the excitation frequency. The coefficient matrices \mathbf{E}_0 , \mathbf{E}_1 , \mathbf{E}_2 , and \mathbf{M}_0 are obtained by assembling the element coefficient matrices showed,

$$\mathbf{E}_0 = \int_{-1}^{+1} \mathbf{B}_1^T \mathbf{C} \mathbf{B}_1 |\mathbf{J}| d\eta, \quad (6)$$

$$\mathbf{E}_1 = \int_{-1}^{+1} \mathbf{B}_2^T \mathbf{C} \mathbf{B}_1 |\mathbf{J}| d\eta, \quad (7)$$

$$\mathbf{E}_2 = \int_{-1}^{+1} \mathbf{B}_2^T \mathbf{C} \mathbf{B}_2 |\mathbf{J}| d\eta, \quad (8)$$

$$\mathbf{M}_0 = \int_{-1}^{+1} \mathbf{N}_u^T \rho \mathbf{N}_u |\mathbf{J}| d\eta, \quad (9)$$

where \mathbf{C} is the elasticity matrix, and \mathbf{B}_1 and \mathbf{B}_2 are matrices that depend only on the geometry of the analyzed element. The static stiffness matrix $\mathbf{K} = \mathbf{D}(\omega = 0)$ for the boundary is defined by setting $\omega = 0$ as:

$$\left(\mathbf{K} - \mathbf{E}_1 \right) \left(\mathbf{E}_0^{-1} \right) \left(\mathbf{K} - \mathbf{E}_1^T \right) - \mathbf{E}_2 + (s-2)\mathbf{K} = 0. \quad (10)$$

Identifying Eq. (10) as a Ricatti equation, it can be solved for \mathbf{K} with the introduction of the Hamiltonian matrix \mathbf{Z} defined as:

$$\mathbf{Z} = \begin{bmatrix} (\mathbf{E}_0)^{-1} (\mathbf{E}_1)^T & -(\mathbf{E}_0)^{-1} \\ -\mathbf{E}_2 + \mathbf{E}_1 (\mathbf{E}_0)^{-1} (\mathbf{E}_1)^T & -\mathbf{E}_1 (\mathbf{E}_0)^{-1} \end{bmatrix}. \quad (11)$$

The stiffness matrix and mass matrix can be written according to [15] as:

$$\mathbf{K} = \mathbf{V}_{21} (\mathbf{V}_{11})^{-1}, \quad \mathbf{M} = ((\mathbf{V}_{11})^{-1})^T \mathbf{m} (\mathbf{V}_{11})^{-1}. \quad (12)$$

Therefore, the dynamic stiffness matrix can be expressed as:

$$\mathbf{D}(\omega) = \mathbf{K} - \omega^2 \mathbf{M}. \quad (13)$$

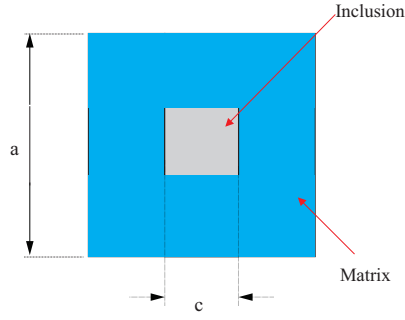


Figure 2. A schematic of a unit cell with square inclusion.

2.1 Phononic Crystal Modelling

This subsection analyzes the PC model and how to apply Bloch-Floquet's theorem for two-dimensional propagation using SBFEM. The model of the first PC unit cell analyzed is shown in Fig.2. It is considered the structure in the plane stress state where the modes are only in the $x - y$ plane (that is a 2D analysis). The PC unit cell is composed of two different materials, one material for the inclusion and another material for the cell matrix.

Analyzing a two-dimensional rectangular mesh, as shown in Fig.3, it can be considered that the indices are related to the location of the nodes, that is, b represents the *bottom* part, l the *left* part, r the *right* part and t the *top* part. Two consecutive indices in a row represent a corner node (e.g., br for bottom right). The index i represents all the *internal* nodes of the structure that do not belong to the external region of the mesh. This study considers that the opposite sides (l/r and b/t) have the same number and location of nodes due to the periodicity conditions.

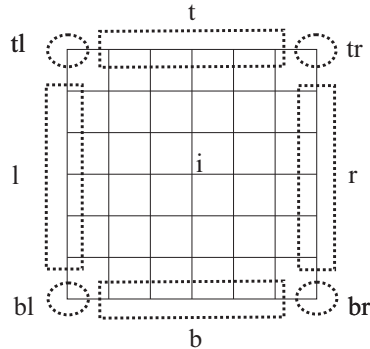


Figure 3. Partitioned nodes for rectangular plate mesh.

The matrix \mathbf{D} may be partitioned between active (master) and internal (slave) degrees-of-freedom (DOFs), according to

$$\begin{bmatrix} \mathbf{D}_{aa} & \mathbf{D}_{ai} \\ \mathbf{D}_{ia} & \mathbf{D}_{ii} \end{bmatrix} \begin{Bmatrix} \mathbf{u}_a \\ \mathbf{u}_i \end{Bmatrix} = \begin{Bmatrix} \mathbf{f}_a \\ \mathbf{f}_i \end{Bmatrix}, \quad (14)$$

where \mathbf{u}_a contains all active DOFs which are in the external region of the mesh, \mathbf{u}_i so-called internal DOFs, and \mathbf{f}_a represents forces acting on nodes related to \mathbf{u}_a . The Eq. (15) shows a dynamic condensation, where it can be found an equivalent dynamic stiffness seen in the boundary of the structure. Since the internal DOFs are condensed, they are used as an intermediate dynamic subsystem, not subject to external forces, but only boundary forces as shown in [16].

$$\mathbf{D}_a = \mathbf{D}_{aa} - \mathbf{D}_{ai} \mathbf{D}_{ii}^{-1} \mathbf{D}_{ia}. \quad (15)$$

Through mathematical manipulations that can be analyzed in [17] the eigenproblem can be assembled as:

$$\begin{bmatrix} \mathbf{T}_L \mathbf{K}_{aa} \mathbf{T}_R & \mathbf{T}_L \mathbf{K}_{ai} \\ \mathbf{K}_{ia} \mathbf{T}_R & \mathbf{K}_{ii} \end{bmatrix} \begin{Bmatrix} \mathbf{u}_c \\ \mathbf{u}_i \end{Bmatrix} = \omega^2 \begin{bmatrix} \mathbf{T}_L \mathbf{M}_{aa} \mathbf{T}_R & \mathbf{T}_L \mathbf{M}_{ai} \\ \mathbf{M}_{ia} \mathbf{T}_R & \mathbf{M}_{ii} \end{bmatrix} \begin{Bmatrix} \mathbf{u}_c \\ \mathbf{u}_i \end{Bmatrix}. \quad (16)$$

With this, the Eq. (16) can be solved by allocating values λ_x and λ_y for the two-dimensional case or λ_x , λ_y and λ_z for the three-dimensional case and consequently for the matrices \mathbf{T}_L and \mathbf{T}_R in the boundary of the irreducible Brillouin zone (IBZ) and determining all eigenvalues ω^2 , thus obtaining the corresponding band diagrams for the PCs.

3 Simulated Phononic Crystal Applications

In this section, it is analyzed the band gaps found in the PCs. The band diagrams were found for a square unit cell with a square inclusion inside. The PC unit cell consists of steel as the inclusion material i , and nylon 66 as the matrix material m , the properties of the materials used are shown in Table 1. The filling fraction is the cross-section area ratio of inclusion and unit cell, i.e., $\bar{f} = c^2/a^2$.

Table 1. Materials of the unit cell (PCs). The unit cell is composed by nylon 66 (matrix m) and steel (inclusion i).

Properties	Value
Young's modulus (E_i, E_m)	193 GPa, 2 GPa
Density (ρ_i, ρ_m)	8030 kg/m ³ , 1000 kg/m ³
Poisson's ratio (ν_i, ν_m)	0.27, 0.45
Filling fraction	11.11%

In order to analyze the responses to different types of discretizations, some studies were carried out. The unit cells of the PCs were discretized and the mesh used for FEM and SBFEM is shown in Fig. 4 (a) and (b), respectively. The filling fraction was equal to 11.11%, where $a = 0.12$ m and $c = 0.04$ m.

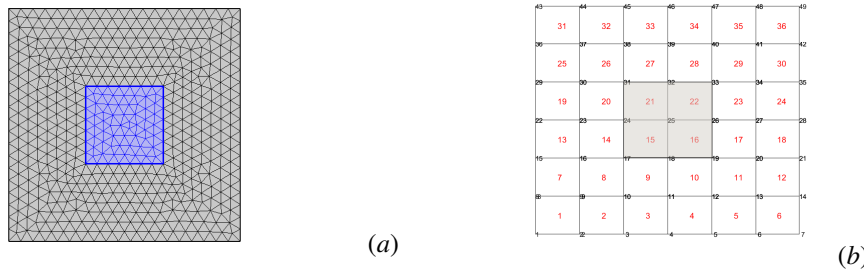


Figure 4. Mesh for unit cell of the phononic crystal. (a) Mesh of the unit cell in COMSOL using $\bar{f} = 11.11\%$. (b) Mesh of the unit cell in the SBFEM using $\bar{f} = 11.11\%$.

The comparison between the elastic band diagram obtained by FEM, SBFEM, and PWE is illustrated in Fig. 5. It is used 36 S elements with 2 DOFs per node for the unit cell for SBFEM and 4770 DOFs for the analysis through COMSOL and triangular finite elements was used. It can be seen in Fig. 5 (a) a band gap in the frequency range of approximately $f = 5.5 - 6$ kHz obtained through FEM and SBFEM. In the Fig. 5 (b), it can be noticed the same band gap region found through the PWE method, which is illustrated through the rectangular area in gray. For the PWE simulations, 49 plane waves were used. In Fig. 6, the FRFs for the complete structure are illustrated. For the analysis of the forced response of the complete structure, 9 unit cells of the PC are used. Here it is used the same excitation points and responses used in the previous example, where H_{11} is for measurement and response at the same node and H_{12} is for measurement and response at different nodes. The band gap regions correspond to those found through the elastic band diagram, and we also noticed a better approximation of the results found by SBFEM with those found by COMSOL because of the refined SBFEM mesh. It can be observed that for higher frequencies, there is still a difference between the methods. Moreover, with the refinement of the SBFEM mesh, the results tend to approach the solution found by COMSOL.

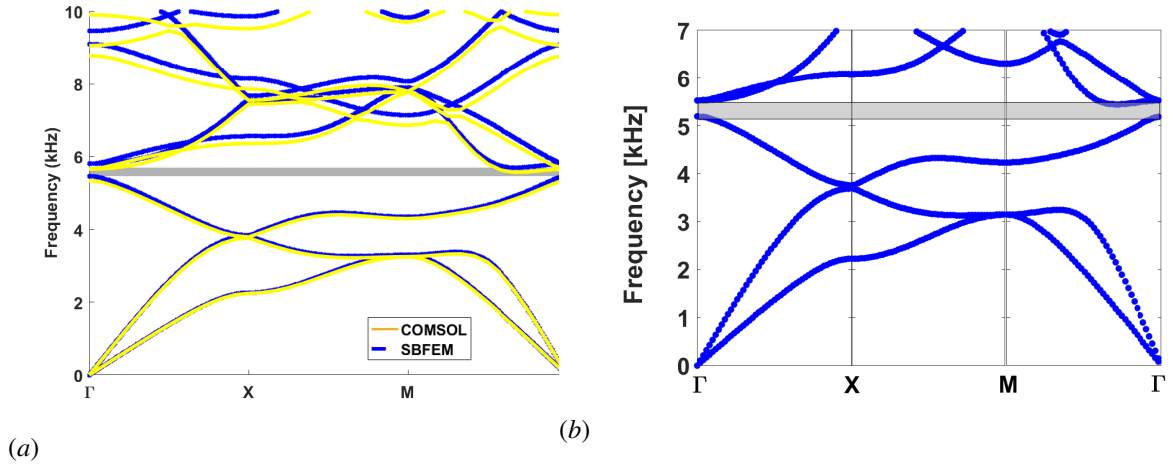


Figure 5. Elastic band structure of steel inclusions in an nylon 66 matrix for a square lattice using $\bar{f} = 11.11\%$. (a) Found through the FEM and SBFEM. (b) Found through the PWE method.

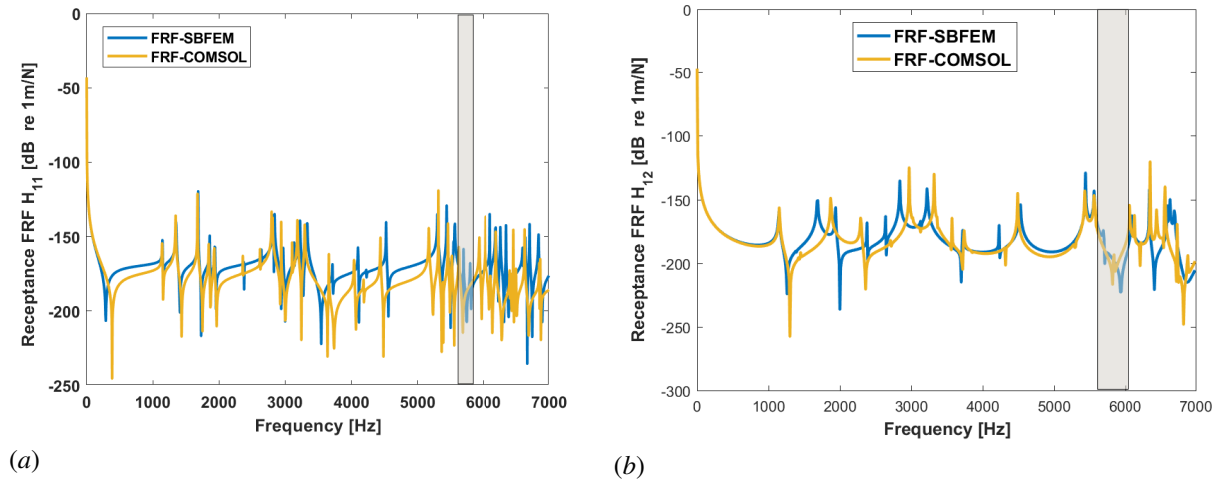


Figure 6. FRF - Receptance for the complete structure. (a) Receptance H_{11} of the complete structure using $\bar{f} = 11.11\%$. (b) Receptance H_{12} of the complete structure using $\bar{f} = 11.11\%$.

4 Conclusions

The elastic band diagrams and the forced response were computed through SBFEM and FEM. A new numerical methodology based on a combination of SBFEM and Floquet-Bloch's theorem was proposed for wave propagation in a 2D phononic crystal. SBFEM, FEM, and PWE method obtained the Bragg band gaps for the cases analyzed, convergence for low frequencies was noted, which was already expected due to the SBFEM approximations.

Acknowledgements. The authors acknowledge the financial support of Federal Institute of Maranhão (IFMA), DMC-FEM-UNICAMP, the Brazilian agencies CAPES (Finance Code 001), CNPq (140783/2017-2, 403234/2021-2, and 405638/2022-1), FAPESP (grant 2018/15894-0), and FAPEMA.

Authorship statement. The authors hereby confirm that they are the sole liable persons responsible for the authorship of this work, and that all material that has been herein included as part of the present paper is either the property (and authorship) of the authors, or has the permission of the owners to be included here.

References

- [1] L. Brillouin. *Wave Propagation in Periodic Structures*. Dover Publications, New York, 1946.

-
- [2] D. J. Mead. A general theory of harmonic wave propagation in linear periodic systems with multiple coupling. *Journal of Sound and Vibration*, vol. 27, n. 2, pp. 235–260, 1973.
- [3] R. M. Orris and M. Petyt. A finite element study of harmonic wave propagation in periodic structures. *Journal of Sound and Vibration*, vol. 33, n. 2, pp. 223–236, 1974.
- [4] F. L. Li, Y. S. Wang, and Z. Q. Wang. Band structure calculations of three-phase phononic crystals based on the boundary element method. *J. Syn. Cryst.*, vol. 38, pp. 1375–1379, 2015.
- [5] Y. Sun, Y. Yu, Y. Zuo, L. Qiu, M. Dong, J. Ye, and J. Yang. Band gap and experimental study in phononic crystals with super-cell structure. *Results in Physics*, vol. 13, pp. 102200, 2019.
- [6] M. S. Kushwaha and P. Halevi. Band-gap engineering in periodic elastic composites. *Applied Physics Letters*, vol. 64, n. 9, pp. 1085–1087, 1994.
- [7] M. M. Sigalas and E. N. Economou. Elastic and acoustic wave band structure. *Journal of Sound and Vibration*, vol. 158, pp. 377–382, 1992.
- [8] Y. F. Wang and Y. S. Wang. Complete bandgaps in two-dimensional phononic crystal slabs with resonators. *Journal of Applied Physics*, vol. 114, n. 4, pp. 043509, 2013.
- [9] Y. Tanaka, Y. Tomoyasu, and S. Tamura. Band structure of acoustic waves in phononic lattices: Two-dimensional composites with large acoustic mismatch. *Physical Review B*, vol. 62, n. 11, pp. 7387, 2000.
- [10] J.-M. Mencik and M. Ichchou. Multi-mode propagation and diffusion in structures through finite elements. *European Journal of Mechanics - A/Solids*, vol. 24, n. 5, pp. 877–898, 2005.
- [11] E. D. Nobrega, F. Gautier, A. Pelat, and J. M. C. D. Santos. Vibration band gaps for elastic metamaterial rods using wave finite element method. *Mechanical Systems and Signal Processing*, vol. 79, pp. 192–202, 2016.
- [12] J. P. Wolf. *Finite-element modelling of unbounded media*. Wiley Chichester, 1996.
- [13] C. Song. *The Scaled Boundary Finite Element Method: Introduction to Theory and Implementation*. Wiley, 2018.
- [14] H. Gravenkamp, S. Natarajan, and W. Dornisch. On the use of nurbs-based discretizations in the scaled boundary finite element method for wave propagation problems. *Computer Methods in Applied Mechanics and Engineering*, vol. 315, pp. 867–880, 2017.
- [15] J. P. Wolf and C. Song. The scaled boundary finite-element method—a primer: derivations. *Computers and Structures*, vol. 78, n. 1–3, pp. 191–210, 2000.
- [16] D. Duhamel, B. R. Mace, and M. J. Brennan. Finite element analysis of the vibrations of waveguides and periodic structures. *Journal of sound and vibration*, vol. 294, n. 1-2, pp. 205–220, 2006.
- [17] B. Mace and E. Manconi. Modelling wave propagation in two-dimensional structures using a wave/finite element technique, 2007.